



Electrodeposition of antimony telluride thin films from acidic nitrate-tartrate baths

Hyunsung Jung, Nosang V. Myung*

Department of Chemical and Environmental Engineering and Center for Nanoscale Science and Engineering, University of California-Riverside, Riverside, CA 92521, United States

ARTICLE INFO

Article history:

Received 31 January 2011

Received in revised form 1 April 2011

Accepted 2 April 2011

Available online 29 April 2011

Keywords:

Antimony telluride

Electrochemical quartz crystal microbalance

Rotating disk electrode

Under-potential deposition

Thermoelectrics

ABSTRACT

Electrochemical quartz crystal microbalance (EQCM) and rotating disk electrode (RDE) techniques were utilized to systematically investigate the electrodeposition of $\text{Sb}_x\text{Te}_{1-x}$ ($0.1 < x < 0.8$). In addition, the effect of applied potential and agitation were correlated to the film composition, crystal structure, and morphology. Although the film composition was independent of the agitation rate, the deposition rate, current efficiency, crystallinity and phase of $\text{Sb}_x\text{Te}_{1-x}$ were all strongly influenced by it. The deposition rate monotonically increased with increases in the rotation rate because of the faster diffusion rate of HTeO_2^+ ions to the cathode. Amorphous thin films were electrodeposited in the absence of agitation, whereas polycrystalline Sb_2Te_3 with elemental Sb and Te were co-deposited at a higher agitation independent of the applied deposition potential.

© 2011 Elsevier Ltd. All rights reserved.

1. Introduction

Antimony telluride (Sb_2Te_3) is a narrow band-gap semiconductor ($E_g = 0.3$ eV) with a rhombohedral crystal structure belonging to the space group $R\bar{3}m$, consisting of alternating layers of Sb and Te perpendicular to the three-fold axis. Due to its unique crystal structure and properties, it has many potential applications including a stable ohmic back contact in high efficiency solar cell devices [1,2], p-type legs for thermoelectric power generators and coolers operating at near room temperature [3–6] and non-volatile phase change memory devices because of its ability to reversibly transform between amorphous to crystalline states [7–9].

Antimony telluride thin films have been synthesized by many different techniques including thermal evaporation [4,10], sputtering [1], molecular beam epitaxy (MBE) [3], metal-organic chemical vapor deposition (MOCVD) [6], hydrothermal/solvothermal synthesis [11,12] and electrodeposition [13–16]. Among them, electrodeposition is an especially attractive method to synthesize thin films, since it is able to rapidly deposit films with controlled morphology, dimension, and crystal structure in a cost effective manner at near ambient conditions. Although the electrodeposition of other chalcogenides such as Bi_2Te_3 , PbTe , CdTe and CdS has been intensively studied [17–27], few works have been reported on $\text{Sb}_x\text{Te}_{1-x}$ electrodeposits. Leimkühler et al. demonstrated the

ability to form $\text{Sb}_x\text{Te}_{1-x}$ thin films on indium tin oxide (ITO) substrates from acidic chloride baths with SbCl_3 and TeO_2 as metal ion precursors [13]. Wang et al. electrodeposited Sb_2Te_3 thin films on Si and Ag substrates from acidic chloride baths, where they observed the effects of the substrates on the microstructures of the $\text{Sb}_x\text{Te}_{1-x}$ thin films [16]. Huang et al. electrodeposited $\text{Sb}_x\text{Te}_{1-x}$ thin films from acidic nitrate baths on physical vapor deposited TiN substrates, where they added sodium citrate to the electrolyte to form Sb-citrate complexes to enhance the Sb solubility in aqueous solution [14].

In this work, detailed electroanalytical studies were performed to understand the deposition mechanism of $\text{Sb}_x\text{Te}_{1-x}$ thin films from acidic nitrate-tartrate baths. The effect of various deposition conditions (i.e. solution composition, agitation, applied potential and operating temperature) on the deposition rate, current efficiency, film composition, morphology, and crystal structure were systematically investigated. The electroactive species and the electrochemical interaction between them were investigated using EQCM. Rotating disk electrodes were employed to investigate the mass transfer effects. The crystal structures and morphologies of the electrodeposited $\text{Sb}_x\text{Te}_{1-x}$ thin films were analyzed by X-ray diffraction (XRD) patterns and scanning electron microscopy (SEM).

2. Experimental

The electrolytes were prepared by separately dissolving TeO_2 (99.9995%, Alfa Aesar, Inc.) in concentrated nitric acid and Sb_2O_3 (99.9%, Fisher Sci.) in L-tartaric acid (99.9%, Fisher Sci.) solutions.

* Corresponding author. Tel.: +1 951 827 7710; fax: +1 951 827 5696.
E-mail address: myung@engr.ucr.edu (N.V. Myung).

Once the oxides were completely dissolved, the solutions were mixed to prepare electrolytes consisting of 0.01 M HTeO_2^+ , 0.02 M SbO^+ , 0.5 M L-tartaric acid and 1 M HNO_3 . The solution pH was approximately 0.08.

All of the experiments were carried out in a 100 ml electrochemical cell with a three electrode configuration with an Ag/AgCl (sat. KCl) electrode and a platinum-coated electrode as the reference and counter electrodes, respectively. A quartz crystal microbalance (QCM) (RQCM, MAXTEX, Inc.) in conjunction with linear sweep voltammetry (LSV) was used to investigate the electroanalytic studies of $\text{Sb}_x\text{Te}_{1-x}$ electrodeposition using polished Au coated quartz crystals (MAXTEX, Inc.) as the working electrodes in the absence of stirring. The operating temperature was varied from 23 °C to 50 °C. The scan rate was fixed at 1 mV/s.

Commercial Au micro electrodes (0.2 cm in diameter, CH Instruments) and in-house fabricated Au-coated copper macro electrodes (1.27 cm in diameter) were used as rotating disk electrodes to determine the mass transfer effects. In addition, $\text{Sb}_x\text{Te}_{1-x}$ films were potentiostatically deposited on Au rotating disk electrodes to analyze the current efficiency and morphology/crystallinity. The mass of each element (i.e. Sb and Te) in the films was determined by atomic absorption spectroscopy (AAS) (AAnalyst 800, Perkin Elmer). The current efficiencies and average partial current densities of H₂, Te, and Sb were calculated based on the reported procedure [14,28]. For example, the current efficiency was determined using Eq. (1), where the mass of each element (i.e. Sb and Te) was determined using AAS.

Current efficiency

$$= \frac{\text{Actual mass of deposits}}{\text{Theoretical mass calculated from Faraday's law}} \times 100(\%) \quad (1)$$

The average partial current densities of the elements (i.e. Te and Sb) were determined from the deposited mass using Eq. (2):

$$i_{\text{Te}} = \frac{\text{mass}_{\text{Te}} n F}{(M W_{\text{Te}} A t)} \quad (2)$$

where i_{Te} is the average partial current density of Te, mass_{Te} is the deposited mass of tellurium, n is the number of electron ($n = 4$ for Te electrodeposition), F is the Faraday constant, A is the deposited area, and t is the deposition time. The average partial current density of H₂ evolution was estimated by subtracting the average partial current densities of the elements from the total average applied current density (Eq. (3)):

$$i_{\text{H}_2} = i_{\text{Tot}} - i_{\text{Te}} - i_{\text{Sb}} \quad (3)$$

where i_{H_2} is the average partial current density of H₂, i_{Tot} is the average total current density, and i_{Sb} is the partial current density of Sb. The film composition of the rotating disk electrodes was also confirmed by energy dispersive spectroscopy (EDS). XRD (X-ray diffractometer, D8 Advanced Diffractometer, Bruker) and SEM (XL30-FEG, Phillips) were utilized to determine the crystal structure and the morphology of the films, respectively.

3. Results and discussion

Sb_2Te_3 , like other chalcogenide compounds (i.e. Bi_2Te_3 and PbTe), is usually electrodeposited under diffusion control [14,17–20] due to the low solubility of HTeO_2^+ ions in the aqueous solutions. To increase the solubility of HTeO_2^+ , the pH of the electrolytes was kept low (pH of 0.08). In addition, a complexing agent such as L-tartaric acid was added to solubilize the SbO^+ ions. Fig. 1 shows the electrochemical quartz crystal microbalance (EQCM) responses during the linear sweep voltammetry (LSV). To determine the deposition potential and deposition rate of the individual elements, three different electrolytes ((1) 0.01 M HTeO_2^+ ,

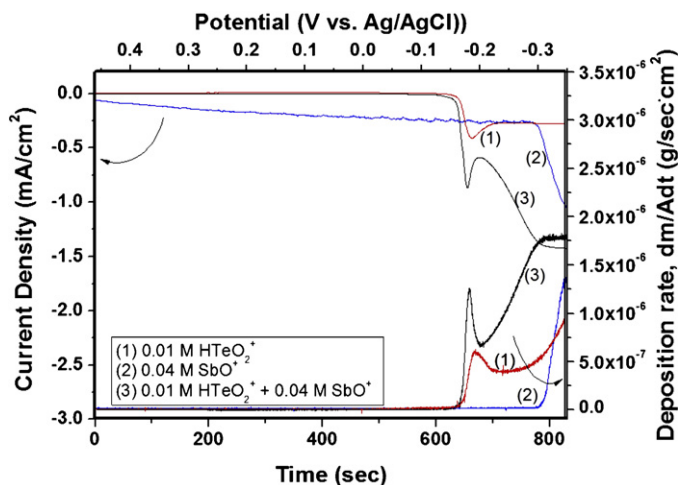
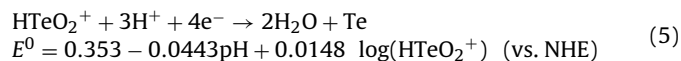


Fig. 1. Deposition rate of electroactive species and current density during linear sweep voltammetry using an electrochemical quartz crystal microbalance system: Solution 1 (red): 0.01 M HTeO_2^+ , 0.5 M L-tartaric acid and 1 M HNO_3 , Solution 2 (blue): 0.04 M SbO^+ , 0.5 M L-tartaric acid and 1 M HNO_3 , Solution 3 (black): 0.01 M HTeO_2^+ , 0.04 M SbO^+ , 0.5 M L-tartaric acid and 1 M HNO_3 . The scan rate and operating temperature were fixed at 1 mV/s and 23 °C, respectively.

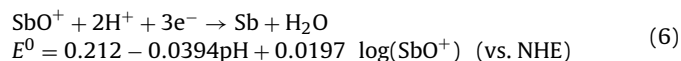
0.5 M L- $\text{C}_4\text{H}_6\text{O}_6$, and 1 M HNO_3 , (2) 0.02 M SbO^+ , 0.5 M L- $\text{C}_4\text{H}_6\text{O}_6$, and 1 M HNO_3 , (3) 0.01 M HTeO_2^+ , 0.02 M SbO^+ , 0.5 M L- $\text{C}_4\text{H}_6\text{O}_6$, and 1 M HNO_3) were studied in the absence of agitation. The EQCM-based deposition rate was calculated from the frequency change in the quartz crystal using Eq. (4), where C_f , Δf , and Δm are the sensitivity factor of the crystal, frequency change and change in mass per unit area, respectively.

$$\Delta f = -C_f \times \Delta m \quad (4)$$

As shown in Fig. 1, the reduction current wave and the increase in frequency of the quartz crystal starting from -0.17 V (vs. Ag/AgCl) in solution A indicated that Te is overpotentially electrodeposited (OPD), which can be described by Eq. (5):



Similarly, the reduction current wave and the increase in frequency of the quartz crystal starting from -0.3 V (vs. Ag/AgCl) in solution B indicated that Sb is OPD, which can be described by Eq. (6):



The electrodeposition of elemental Te and Sb thin films from solutions A and B, respectively, were confirmed by AAS analysis.

Underpotential deposition (UPD) of Sb on OPD Te was observed by comparing the LSVs from solutions A and C. Since solution C contains both HTeO_2^+ and SbO^+ ions, whereas solution A contains only HTeO_2^+ ions, the difference in current densities between the LSVs at the applied potential ranged from -0.17 V to -0.3 V vs Ag/AgCl can be attributed to the UPD deposition of Sb on Te to form Sb_2Te_3 (Eq. (7)).



Unlike the OPD of Sb, the UPD of Sb on Te can occur at lower applied potentials than the OPD of Sb because of the negative Gibbs free energy of Sb_2Te_3 formation ($\Delta G_f = -57.5$ kJ/mol) (Eq. (7)), where the Sb_2Te_3 intermetallic compound is formed by alternating

Download English Version:

<https://daneshyari.com/en/article/189491>

Download Persian Version:

<https://daneshyari.com/article/189491>

[Daneshyari.com](https://daneshyari.com)